Journal of Analytical & Bioanalytical Techniques

Kristy L.Kounovsky Shafer et al., J Anal Bioanal Tech 2021, 12:2

Research Article Open Acces

Determining the Effective Electrophoretic Mobility of Fluorescently Labeled Microspheres in Microchannels in a Dynamic Range of Ionic Strength Conditions

Bryant Menke, Samantha Rau, Anna Ripp and Kristy L. Kounovsky Shafer*

Department of Chemistry, University of Nebraska-Kearney, Kearney, NE, USA

ABSTRACT

Nano coding, a system for genome analysis, utilizes electro osmosis and electrophoresis to park DNA molecules in molecular gates. Understanding how electro osmotic and electrophoretic mobilities vary due to surface charge of the device will enable better devices to be developed for Nano coding or other genome analysis platforms. Using a current monitoring method, the surface charge was determined for three different plasma treatments of poly (dimethylsiloxane) (PDMS). Next, the effective electrophoretic mobility of negatively charged fluorescently labeled microspheres was measured for a dynamic range of ionic strength solutions (0.500 – 18.00 mM). As the ionic strength decreased, the effective electrophoretic mobility (or net mobility) decreased or moved in the opposite direction due to electro osmosis. For all three plasma treatments, the lower ionic strength solutions (0.500 and 1.000 mM) were dominated by electro osmosis. Electro osmosis dominated at 2.00 mM for the two highest surface charges. The experimental net mobility was compared to theoretical considerations, utilizing the Pitts equation for electrophoretic mobility and the Stellwagen equation for electro osmotic mobility. Both theoretical and experimental show the net mobility decreased as the ionic strength decreased.

Keywords: Electro osmosis; Electrophoresis; Fluorescent microspheres; Low ionic strength solutions

Introduction

A larger number of bases are varied in the human genome from structural variation compared to single nucleotide polymorphisms [1,2] and have been linked to different diseases [3,4]. Physical mapping platforms, such as Nano coding [5-7] and Optical Mapping [8-10], identify large variations (5 kb to hundreds of kilobases to mega base in size) in different genomes and aids in assembling sequence information as a hierarchal scaffold [11]. In Nano coding, DNA molecules were labeled at sequence specific locations by nicking the DNA with a nicking enzyme and incorporating fluorescently labeled nucleotides [5-7] and then loaded into micro channels via capillary action to populate the micro channels. A low electric potential was applied to park DNA in molecular gates, which were abutted against the Nano slits. The electric potential was increased to synchronously load DNA molecules into Nano slits then the electric field was turned off when the molecule spans the Nano slit with each end in opposing micro channels. The process of parking DNA in the molecular gates required both electro osmosis and electrophoresis. Understanding how the surface charge of a poly (dimethylsiloxane) (PDMS) device plays a role in the effective electrophoretic mobility, or net mobility, in different ionic strengths will aid in understanding and enable optimization of electro osmosis and electrophoresis in micro channels.

Under an applied electric field, analytes, such as DNA or negatively charged latex microspheres, were affected by electro osmotic and electrophoretic mobilities, which affect the net mobility [6]. Electrophoresis occurs when the analyte, in this case a negatively charged analyte, has an electric field applied and moves towards the anode or positive electrode. Electro osmosis occurs when there are fixed charges on the surface such as silanol groups on PDMS. PDMS is a silicon-based inorganic polymer (C2H6OSi) n [12] that is polymerized with two components are mixed and heated. PDMS's surface can be modified using oxygen plasma treatment [8,9], surface segregating smart polymers [13], or corona discharge [14,15] to impart surface charge. In our case, a PDMS device was plasma treated to impart negative charge on a surface. For electro osmosis, cations are attracted to the negatively charged surface and once the electric field is applied the cations move towards the cathode pulling water molecules along [16,17]. Theoretically, electro osmosis increases as the ionic strength decreases [18,19]. Within the micro channels, electro osmosis and electrophoresis oppose each other, which cause the net mobility of the analyte to be perturbed.

Kounovsky-Shafer et al. developed parking and loading of DNA molecules in molecular gates using both electro osmosis and electrophoresis [6]. In these experiments, the net mobility of DNA and the type of loading was determined in a dynamic range of low ionic strength solutions in a micro channel Nano slit device. DNA molecules either migrated through acute (electro osmosis and electrophoresis present, high ionic strength solutions) or obtuse loading (electrophoretic mobilities dominate, low ionic strength solutions). In order to tease out what was happening during loading, a simpler experiment was utilized that had the electrode in the middle rather than in opposite corners and compared two different ionic strength solutions in just a micro channel to see the migration of the DNA molecules. At a low ionic strength solution (0.51 mM), DNA migration was dictated by electro osmosis, as electro osmotic mobilities were greater than electrophoretic mobilities, which caused DNA to migrate "backwards". At a higher ionic strength solution (8.5

***Corresponding author:** Kristy LKS, Department of Chemistry, University of Nebraska-Kearney, Kearney, NE, USA, E-mail: kounovskykl@unk.edu

Received: January 19, 2021; **Accepted:** February 02, 2021; **Published:** February 09, 2021.

Citation: Kristy LKS, Menke B, Rau S, Ripp A (2021) Determining the effective electrophoretic mobility of fluorescently labeled microspheres in microchannels in a dynamic range of ionic strength conditions. J Anal Bioanal Tech 12: 427.

mM), DNA migration was in the forward direction or electrophoretic mobilities dominated causing the negatively charged DNA molecule to migrate towards the positive electrode (anode). However, these experiments only utilized one plasma treatment. Additionally, there were only two ionic strength solutions that were compared inside a micro channel. Furthermore, there is a lack of knowledge of how the surface charge of PDMS affects the net mobility of particles in low ionic strength solutions. In another study by Lallman et al., electro osmotic and electrophoretic mobility was measured in a dynamic range of low ionic strengths in gels, but did not examine what happened in micro channels [20]. Therefore, new experiments must be done to understand how the net mobility changes in a dynamic range of ionic strength solutions with different surface charges (PDMS).

This paper examined how modifying the surface charge through different plasma treatments of PDMS devices affected the net mobility of fluorescent micro particles in a dynamic range of low ionic strength solutions. The objective for this study was to investigate how a range of different surface charges affected the net mobility of these particles, as well as changing the ionic strength of the solution. By decreasing the ionic strength and increasing the negative surface charge on the PDMS, electro osmosis became more prominent. In addition, the mobility was compared to a theoretical model for electrophoretic mobility (Pitts) and electro osmotic mobility to determine how the net mobility changed as the ionic strength decreased.

Materials and Methods

Materials

Ultimaker printers (2+ and 3), polylactic acid (PLA) filament and acrylonitrile butadiene styrene (ABS) filament were purchased through Dynamism (Chicago, IL) or fbrc8 (Bartlett, TN). SU8 2005 and SU8 developer was purchased through MicroChem (Westborough, MA). Sodium chloride was purchased through Sigma Aldrich (Saint Louis, MO). The Fluospheres (1.0 μm carboxyl terminated yellow-green fluorescent microspheres) and isopropyl alcohol were purchased through Thermo Fisher Scientific (Waltham, MS).

Measurement of surface charge

A channel (1.37 mm width x 0.41 mm height x 9.80 mm length) with two ports (2.5 mm diameter x 6.0 mm height) was designed on AutoCAD, converted to a printable file on Cura, and printed using a converted Ultimaker 2+ 3D printer. A 101.6 mm silicon wafer (University wafer, South Boston, MA) was glued onto the hotbed of the Ultimaker 2+ using a glue slick and the printer printed the channels and ports directly onto the wafer using ABS (Figure S1). PDMS was poured onto the wafer and baked at 35°C for at least one day. There were three different plasma treatments: (1) 36 s O2 plasma, 15% power; (2) 18 s O2 plasma, 15% power; and (3) 54 s O2 plasma, 15% power. The channels, after plasma treatment, were placed in a conical tube of distilled water.

A plasma treated coverslip (8 min, 100% power) was attached to the PDMS device. Using a similar setup to Mampallil et al. and Dasgupta et al., a 25 mM and 50 mM NaCl solutions were added to the two ports and a potential was applied (105.7 V) [21,22]. The distance between electrodes in the experiment was 11 mm-15 mm. A 9.99 k□ resistor (R) was used and the potential drop (V) was measured across the resistor and converted to current using V=ICR to measure the time dependence of the current (IC) in the channel. When the current plateaued, the displacement time (td) was determined.

Sample preparation, imaging and analysis

A series of five different ionic strength solutions were made using NaCl: 18.00, 9.000, 2.000, 1.000 and 0.500 mM. These solutions were used make dilutions of the fluorescent microparticle solutions and immersed the PDMS device (fabrication of the SU8 device and PDMS replica are in the SI Methods section) [23,24].

Glass coverslips (22 mm x 22 mm, Fisher Scientific) were plasma treated for 8 min on both sides and were placed in a 50 mL conical tube filled with ethanol. Coverslips and PDMS were dried and then attached. The glass coverslip was attached to a 3D printed holder a rectangle with a square hole that was printed with an Ultimaker 3 with wax (Figure 1). The holder had platinum wires attached to apply a potential across the device. Microsphere solution was loaded into the PDMS device through capillary action and the device was immersed in corresponding NaCl solution. An electric field (Kepco bipolar power supply/amplifier; Flushing, NY) was applied to the device and the particles were imaged on an Olympus Fluoview FV3000 confocal microscope (Tokyo, Japan). Image files were imported into Image J and the particle location was tracked and converted into mobility.

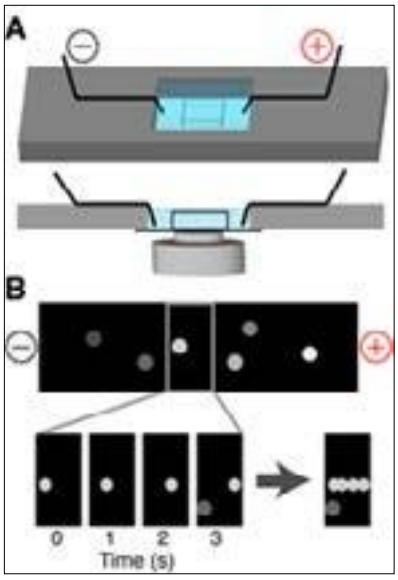

Figure 1. A schematic of the system. (A) A 3D printed holder was made using an Ultimaker 3 printer and platinum wires were attached to the holder to apply an electric field. A PDMS device was attached to a glass coverslip and the glass coverslip was attached to the holder using wax. The fluorescently labeled 1 mm microspheres were loaded into the microchannel through capillary action and then the PDMS device was immersed in the same buffer as the fluorescently labeled polystyrene beads. The concentration of the particles did not noticeably change inside the microchannels with the addition of buffer, as we measured the movement of the particles in the middle of the channel. An electric field was applied, and the beads were monitored using a fluorescence microscope. (B) Images were captured, and the position of the microspheres was determined using ImageJ over time. An image of the particles' migration is shown by compiling the maximum intensity of each image into one image.

Results and Discussion

Developing 3D printed channels to measure surface charge

In order to measure the surface charge of PDMS devices, a two-port device with a channel connecting the two ports needed to be fabricated. Fabrication of large features using photolithography is time-consuming and costly. Therefore, a new method to produce channels with ports was devised using 3D printing. The channels with ports were designed in AutoCAD 2018 and converted to gcode file using Cura software. Adhering a PDMS device onto a glass surface required a smooth PDMS surface on either side of the channel. Because making the surface uniform around the 3D printed channel was difficult, the 3D printed channel was printed onto a silicon wafer. The wafer was attached to the 3D printer bedplate using a glue stick prior to printing and the features were printed with ABS.

In order to make a replica of the channels, PDMS was poured onto the wafer and baked, removed, and plasma treated for 18, 36, or 54 s. These PDMS devices were placed on a glass coverslip that was treated using oxygen plasma (8 min., 100% power). Using the method developed by Mampallil et al., Dasgupta et al. and Huang et al., the surface charge was measured [21,22,25]. A different solution of sodium chloride was added to each port (50 mM and 25 mM), platinum wires were placed into each port, and a potential was applied (Figure S2). The potential drop (V) across the 9.99 kΩ resistor (R) was measured and converted to a current (IC) using V=IcR. During the experiment, the displacement of solutions (td) was completed when the data plateaus. From td, we can calculate the initial time the fluid starts to replace the initial solution (t0) [22].

$$t(\lambda) = t_0\left[\frac{P-Q}{Q^2}\right]\ln(1-Q\lambda) + \frac{P}{Q}\lambda \quad (1)$$

Where we calculated t0 using the displacement time where λ=1, which means t_d=t(1), P=1-c, c=C_*i*C_f,Ci is the initial concentration in the channel and Cf is the final concentration in the channel, Q=1-c^(2/3) g_r [22]. g(σ,κ) is a function of σ and κ (the inverse Debye length $g_r = \frac{g(\sigma,\kappa_1)}{g(\sigma,\kappa_2)}$ and κ=(2000F^2 I/εk_B T)^(1/2). κ1 and κ2 represent the inverse Debye length of the two different concentrations. κ1 is the final concentration and κ2 is the initial concentration. With small zeta potentials, g_r=g(σ,κ_1)/g(σ,κ_2) so g_r= 1 . F is Faraday's constant, kb is Boltzmann constant, and T is temperature and ε is the relative permittivity of the electrolyte. The surface charge can be calculated using the following equation [22].

t_0=(-ηκ_2 L^2)/σg(σ,κ_2) V^(-1) (2)

Where η is dynamic viscosity, L is the length, σ is surface charge density, and g(σ, κ) =1 at small zeta potential values. td was measured from the graph in Figure S3. From the displacement of solution, the surface charge was calculated using Eq. (1) and (2) for each concentration (Table S1). For the different plasma treatments (18, 36, and 54 s), the surface charge was -18 ± 5, -22 ± 4, and -29 ± 4 mC/m2. As expected, the increase in length of plasma treatment increased the surface charge of the PDMS.

The surface of the 3D printed channel (Figure S1D) has bumps due to printing. The height of these bumps is ~6 μm tall; whereas, the height of the channel is 410 μm tall. The surface roughness (Ra) and the root-mean-square roughness (Rq) of the 3D printed channel and SU8 channel (1.4 mm wide x 4 μm high, not used in the experiments) were measured with an Alpha Step 500 profilometer (KLA, Milpitas, CA). The average roughness (Ra) for the SU8 channel was 0.3721 μm and the 3D printed channel was 1.4581 μm (Table S2). The 3D printed channel was rougher than the SU8 channel; however, the fabrication of the 3D printed channel is faster (4.2 min printing time for one device) and easier (no post processing) compared to SU8.

Fabrication of microfluidic devices to measure net mobility of particles

Microfluidic devices were fabricated through photolithography. SU8 2005 was poured onto a silicon wafer and spin coated in a Laurell Tech spin coater and exposed using UV light from a Strata gene Strata linker 1800. A mixture of 10:1 Sylgard 184 prepolymer to platinum catalyst ratio were mixed with a Kitchen Aid hand mixer and then poured the wafer and baked (60°C) overnight. The solidified PDMS was removed then plasma treated for 18, 36 or 54 s and stored in distilled water until use.

PDMS devices were attached to plasma cleaned glass coverslips to form the micro channel and then the glass was attached to a 3D printed holder with wax. The fluorescent micro particle solution was loaded into the micro channel via capillary action and the corresponding ionic strength solution (I) was added to immerse the PDMS device in solution (Figure 1). The holder has platinum wires attached, so a potential could be applied across the micro channel and imaged using an Olympus Fluoview FV3000 confocal laser scanning microscope. The particles collected in the videos (videos S1 and S2) were tracked to measure the mobility. Additionally, the images from a video were compiled with the maximum intensity for each pixel was shown in one image to see the migration of the particles (video 2). In order to show that the electric field was driving the particles, a control experiment was completed (video S3, Figure S4) to show the migration was due to the electric field. In 1.000 mM sodium chloride solution (Figure 2A, video S1), the yellow-green carboxyl terminated fluorescent micro particles (1 μm) were moving towards the negative electrode which indicated electro osmosis dominated. In 9.000 (Figure. 2B, video S2) and 18.00 mM sodium chloride solution, the negatively charged particles migrated toward the positive electrode indicating electrophoresis dominated. The net mobility of the particles was measured using ImageJ for each ionic strength solution and plasma treatment. Net mobility (μnet) is comprised of electrophoretic (μnet) and electro osmotic (μnetEOF) mobility.

μ_net=μ_EF+μ_EOF (3)

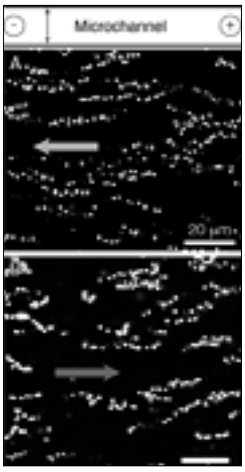

Figure 2. Individual images are compiled into one image using the maximum intensity to show the migration of fluorescently labeled microspheres. Once the microspheres were loaded into the

microchannel, the PDMS device was immersed in the same buffer. Images of the fluorescently labeled beads were taken over time. (A) The beads were diluted in 1.000 mM NaCl solution and were loaded into a device (36 s plasma treatment). The negatively charged beads moved towards the negative electrode indicating electroosmotic mobility dominated (light gray arrow). (B) In this image, the beads were diluted in 9.000 mM NaCl solution, so it had higher ionic strength than in Figure 2A. At higher ionic strength solutions, the negatively charged particles migrated towards the positive electrode (anode) indicating electrophoretic mobility dominated (dark gray arrow). The plasma treatment was 36 s.

The electrophoretic and electro osmotic mobility may be in the same direction or opposite directions depending on the charge of the ion. In our case, the electro osmotic mobility was in the opposite direction of electrophoretic mobility, so the net mobility will be less than the electrophoretic mobility. Since electrophoretic mobilities are vector quantities, the electro osmotic mobility is subtracted from the electrophoretic mobility.

In our case, the surface charge of the device was negatively charged, so the positive charges in the solution were near the surface and migrated towards the negative electrode and carried water to induce electro osmosis. When the negatively charged particles migrated towards the negative electrode, this indicated electro osmosis dominated. If the negatively charged particles migrated towards the positive electrode, this indicated that electrophoresis dominated. The particles mobility was tracked using Image in Figure 3. For 18 s plasma treated device (surface charge=-18 ± 5 mC/m2), electrophoretic mobility (positive mobility) dominated at I>1.000 mM. Only the lowest ionic strength was dominated by electro osmotic mobility. For 36 and 54 s plasma treated devices (surface charge of -22 ± 4 mC/m2 and -29 ± 4 mC/m2, respectively), electrophoresis dominated at I>9.000 mM. In both plasma treatments, electro osmosis dominated at the lower ionic strength solutions. In order to view the data qualitatively, Figure 3 data was shown with an arrow either gray (electro osmotic dominated) or black (electrophoretic dominated) in Figur 4. The smaller the arrow the smaller the net mobility and the bigger the arrow the larger the mobility. Electrophoresis prevailed at I=9.000 and 18.00 mM for all three plasma treatments. Only the smallest surface charge (18 s, -18 mC/m2) had electrophoresis dominating at I=1.000 and 2.000 mM and the other two plasma treatments were dominated by electro osmosis. At 0.500 mM ionic strength for all three surfaces, electro osmotic mobility predominated. An increase in surface charge, increased electro osmosis which overtook electrophoresis at lower ionic strength solutions.

Comparing experimental and theoretical mobility

In Figure 5, the experimental net mobility was plotted against ionic strength and compared to the theoretical net mobility. The electrophoretic equation (Pitts) utilized Debye-Hückel limiting laws [26] for ions of finite size to determine the conductance of an ion [27]. The simplified electrophoretic equation for mobility (μEF) is [27]

$$\mu_{EF} = \mu_i^o - \left(3.125 \times 10^{-4} z_i + \frac{0.3291 |z_i| 2q\mu_i^o}{1+q^{\frac{1}{2}}}\right) \times \frac{I^{\frac{1}{2}}}{1+Bd_1 I^{\frac{1}{2}}} \quad (4)$$

where μ_i^o is the mobility at zero ionic strength, zi is the charge of the anion, I is ionic strength, B is a constant (0.3291 A-1M-1/2), q is the electrolyte type parameter, d1 is the distance between the counterion and analyte. This equation was simplified by Li et al. and Stellwagen et al. [18,28]

$$\mu_{EF} = \mu_i^o - c_1 \left[\frac{I^{\frac{1}{2}}}{\left(1+c_2 I^{\frac{1}{2}}\right)}\right] \quad (5)$$

Where c2 is an adjustable constant and c1 is the Onsager limiting slope. In order to approximate the electrophoretic mobility in the Pitts equation, the free solution mobility was set at 2.3 x 10-4 cm2/Vs, the Onsager limiting slope was approximated to 11.4, and c2 was set to 3.8.

The electro osmotic mobility (μEOF) is [29]

$$\mu_{EOF} = \frac{\sigma}{\eta\kappa' I^{\frac{1}{2}}} \quad (6)$$

Where κ' is the inverse Debye length without ionic strength. In order to compare the experimental net mobility to theoretical net mobility, the electrophoretic and electro osmotic mobilities were combined (Eq 3). In Figure 5, the experimental data (black circles, 36 s plasma treatment; gray squares, 18 s; white diamonds, 54 s) was paired with the theoretical net mobility. In Figure 5A, the electro osmotic mobility was calculated using the surface charge determined from the current experiment for each device and combined with electrophoretic mobility to determine the net mobility using Eqs. (3, 5, and 6). The theoretical prediction for net mobility was closest to the 18 s plasma treatment. For the other two plasma treatments, the theoretical predication was not as close. In Figure 5B, a dynamic range of surface charges were used (-100, -80, -40, and -22 mC/m2) and plotted with the experimental data. When the surface charges were expanded, the -100 mC/m2 surface charge overlaid the 54 s plasma treated device and -80 mC/m2 surface charges overlaid the 36 s plasma treated device. Given the experimental values of surface charge (-22 and -29 mC/m2), the data was below the theoretical predicted values. At lower ionic strength solutions, the surface charge may play a larger role in electro osmotic mobility, which may be why the data aligned better with higher surface charges.

Conclusion

In summary, the net mobility of fluorescent microspheres was determined for a dynamic range of ionic strengths in three different PDMS devices with different surface charge. As the ionic strength decreased, the net mobility slowed down or switches directions due to the increase in electro osmotic mobility. The higher surface charge caused the net mobility of the negatively charged particles to be higher due to the electro osmotic mobility being very small. The lowest surface charge (-18 mC/m2) only had one ionic strength where the particles moved towards the negative electrode due electro osmosis. For the other two surface charges (-22 and -29 mC/m2), there were three ionic strengths that had electro osmosis dominating the direction of the particle. At low ionic strength solutions, the surface charge may be playing a larger role in the magnification of electro osmosis. More theoretical work needs to be done to be able to predict what is happening at the lower ionic strength solutions. Additionally, future theoretical models could be developed to translate the electro kinetic parameters of PDMS replicas of 3D printed channels compared to traditional photolithographic channels, especially the increase of surface roughness from using 3D printed devices.

The data and information gained in this study on how these mobilities vary under confinement in micro channels will help understand how electro osmosis and electrophoresis interact in low ionic strength solutions, which are required for Nano coding. The work from this study on how net mobility varies with surface charge and ionic strength can be utilized to harness electro osmosis and electrophoresis in Nano coding to park DNA molecules in molecular gates.

Acknowledgements

The National Center for Research Resources (NCRR; 5P20RR016469) and the National Institute for General Medical Science (NIGMS; 8P20GM103427), a component of the National Institutes of Health (NIH) and the University of Nebraska at Kearney (UNK) Summer Student Research Program (SSRP) and Undergraduate Research Fellowship (URF) funded this research. Nebraska Research Initiative for equipment used in this project.

Conflict of interest

The authors have declared no conflict of interest.

References

1. Genomes Project C, Auton A, Brooks LD, Durbin RM, Garrison EP, et al. (2015) A global reference for human genetic variation. Nature.526 (7571) : 68-74.
2. Conrad DF, Pinto D, Redon R, Feuk L, Gokcumen O, et al. (2010) Origins and functional impact of copy number variation in the human genome. Nature. 464:704-712.
3. Chen C, Qiao R, Wei R, Guo Y, Ai H, et al. (2012) A comprehensive survey of copy number variation in 18 diverse pig populations and identification of candidate copy number variable genes associated with complex traits. BMC Genomics. 13: 733.
4. Stefansson H, Meyer-Lindenberg A, Steinberg S, Magnusdottir B, Morgen K, et al. (2014) CNVs conferring risk of autism or schizophrenia affect cognition in controls. Nature. 505:361-366.
5. Kounovsky-Shafer KL, Hernandez-Ortiz JP, Jo K, Odijk T, de Pablo JJ, Schwartz DC, et al. (2013) Presentation of large DNA molecules for analysis as nanoconfined dumbbells. Macromolecules. 46:8356-8368.
6. Kounovsky-Shafer KL, Hernandez-Ortiz JP, Potamousis K, Tsvid G, Place M, et al. (2017) Electrostatic confinement and manipulation of DNA molecules for genome analysis. Proc Natl Acad Sci U S A. 114:13400-13405.
7. Jo K, Dhingra DM, Odijk T, de Pablo JJ, Graham MD, et al. (2007) A single-molecule barcoding system using nanoslits for DNA analysis. Proc Natl Acad Sci USA. 104:2673-2678.
8. Dimalanta ET, Lim A, Runnheim R, Lamers C, Churas C, et al. (2004) A microfluidic system for large dna molecule arrays. Anal Chem. 76:5293-5301.
9. Teague B, Waterman MS, Goldstein S, Potamousis K, Zhou S, et al. (2010) High-resolution human genome structure by single-molecule analysis. Proc Natl Acad Sci USA. 107:10848-10853.
10. Zhu Y, Xu J, Sun C, Zhou S, Xu H, et al. (2015) Chromosome-level genome map provides insights into diverse defense mechanisms in the medicinal fungus Ganoderma sinense. Sci Rep. 5:11087.
11. Zhou S, Wei F, Nguyen J, Bechner M, Potamousis K, et al. (2009) A single molecule scaffold for the maize genome. PLoS Genet. 5(11):e1000711.
12. Allcock HR. (1992) Rational design and synthesis of new polymeric material. Science. 255 (5048) :1106-1112.
13. Gokaltun A, Kang YBA, Yarmush ML, Usta OB, Asatekin A, et al. (2019) Simple surface modification of poly (dimethylsiloxane) via surface segregating smart polymers for biomicrofluidics. Sci Rep. 9:7377.
14. Haubert K, Drier T, Beebe D. (2006) PDMS bonding by means of a portable, low-cost corona system. Lab Chip. 6:1548-1549.
15. Gokaltun A, Yarmush ML, Asateki A, Usta OB (2017) Recent advances in nonbiofouling PDMS surface modification strategies applicable to microfluidic technology. Technology (Singap World Sci). 5:01-12.
16. Himenz PC Rajagopalan R (1977) Principles of Colloid and Surface Chemistry. (3rdedn), Marcel Dekker, New York, Basel.
17. Adamson AW, Gast AP (1967) Physical Chemistry of Surfaces. (6thedn) A Wiley-Interscience Publication, New York .
18. Stellwagen E, Stellwagen NC (2003) Probing the electrostatic shielding of DNA with capillary electrophoresis. Biophys J. 84:1855-1866.
19. Tandon V, Bhagavatula SK, Nelson WC, Kirby BJ (2008) Zeta potential and electroosmotic mobility in microfluidic devices fabricated from h`ydrophobic polymers: 1. The origins of charge. Electrophoresis. 29:1092-1101.
20. Lallman J, Flaugh R, Kounovsky-Shafer KL (2018) Determination of electroosmotic and electrophoretic mobility of DNA and dyes in low ionic strength solutions. Electrophoresis. 39:862-868.
21. Dasgupta S, Buhagat AAS, Horner M, Papautsk I, Banerjee RK (2018) Effects of applied electric field and microchannel wetted perimeter on electroosmotic velocity. Microfluidics and Nanofluidics. 5:185-192.
22. Mampallil D, van den Ende D, Mugele F (2010) A simple method to determine the surface charge in microfluidic channels. Electrophoresis. 31:563-569.
23. Gupta A, Place M, Goldstein S, Sarkar D, Zhou S, et al. (2015) Single-molecule analysis reveals widespread structural variation in multiple myeloma. Proc Natl Acad Sci USA. 112:7689-7694.
24. Gupta A, Kounovsky-Shafer KL, Ravindran P, Schwartz D (2016) Microfluidics and Nanofluidics. 20: 1-14.
25. Huang Z, Gordon MJ, Zare RN (1988) Current-monitoring method for measuring the electroosmotic flow rate in capillary zone electrophoresis. Anal Chem 60:1837-1838.
26. Onsager L (1927) Physikalische Zeitschrift. 27: 388-392.
27. Pitts E (1953) Proc. Royal Soc. London, Series A: Mathematical, Physical Eng. Sci. 217: 43-70.
28. Li D, Fu S, Lucy CA (1999) Anal Chem 71: 687-699.
29. Stellwagen E, Stellwagen NC (2002) The free solution mobility of DNA in Tris-acetate-EDTA buffers of different concentrations, with and without added NaCl. Electrophoresis 23:1935-1941.